Cardiovascular MRI in Practice

Cardiovascular MRI in Practice

A Teaching File Approach

By

John D. Grizzard, MD
Assistant Professor, Department of Radiology, Director, Non-invasive Cardiovascular Imaging, VCU Medical Center, Richmond, VA, USA

Robert M. Judd, PhD
Associate Professor, Department of Medicine and Radiology, Co-Director, Duke Cardiovascular Magnetic Resonance Center, Duke University Medical Center, Durham, NC, USA

Raymond J. Kim, MD
Associate Professor, Department of Medicine and Radiology, Co-Director, Duke Cardiovascular Magnetic Resonance Center, Duke University Medical Center, Durham, NC, USA

Springer

John D. Grizzard, MD
Assistant Professor, Department of Radiology, Director, Non-invasive Cardiovascular Imaging, VCU Medical Center, Richmond, VA, USA

Robert M. Judd, PhD
Associate Professor, Department of Medicine and Radiology, Co-Director, Duke Cardiovascular Magnetic Resonance Center, Duke University Medical Center, Durham, NC, USA

Raymond J. Kim, MD
Associate Professor, Department of Medicine and Radiology, Co-Director, Duke Cardiovascular Magnetic Resonance Center, Duke University Medical Center, Durham, NC, USA

ISBN 978-1-84800-089-6 e-ISBN 978-1-84800-090-2
DOI 10.1007/978-1-84800-090-2

Library of Congress Control Number: 2008921382

Printed on acid-free paper

9 8 7 6 5 4 3 2 1

springer.com

To my three sons– Patrick, Michael, and Kevin– with love. And to Louisa for her encouragement.

– JDG

To my immediate family—Sue, Matt, Kevin, and Elizabeth, and to the grandfather I never met, Herbert Alvin Judd, who left a wife and four children when he died of heart disease at the age of 46.

–RMJ

To Enn-ling, Alison, and 'Kiwi'—my treasures.

–RJK

And to those patients whose heart or vascular disease is portrayed herein with the hope that this endeavor may ultimately prove helpful to other patients and the physicians involved in their care.

–JDG, RMJ, RJK

Preface

Cardiovascular MR imaging has become a robust, clinically useful modality, and the rapid pace of innovation and important information it conveys have attracted many students whose goal is to become adept practitioners. In turn, many excellent textbooks have been written to aid this process. These books are necessary and useful in helping the student learn the underlying pulse sequences used in CMR, as well as the imaging findings in a variety of disorders. However, one of the difficulties inherent in learning CMR from a book is that the printed format is not the ideal medium to display the dynamic imaging that comprises a typical CMR case. For instance, it may be difficult to perceive focal areas of wall motion abnormality on serial static pictures, but these abnormalities are often easily seen on cine loops. One might say that trying to learn CMR solely from a standard textbook with illustrations is like trying to learn to drive by looking at snapshots obtained through the windshield of a moving car. The learner needs to see the cardiac motion and decide if it is normal or abnormal; he or she needs to be in the driver's seat. An additional limitation of the available textbooks on CMR is that while they often have superb illustrations of abnormal findings, these images have been preselected. In transitioning to the "real world," the challenge is for the student to be able to find the pathology. Therefore, ideally the student should make an initial attempt at deciding what is normal and abnormal in a given scan, as it is our experience that it is not uncommon for patients to leave the CMR facility with a diagnosis that differs importantly from the original indication for the scan. To do this successfully, the student needs to see the entire scan, with the mistakes and inconclusive images included, rather than attempt to become proficient in CMR based solely on preselected images that simply support the final diagnosis.

This book represents a new and different way of learning CMR. The entire project is encoded on a single (dual-layer) DVD as a series of Web pages that can be displayed offline in any Web browser (e.g. Internet Explorer, Firefox, Safari). Unlike previous CMR textbooks, which typically contain a few preselected views for each case, the DVD contains the *entire scan* for each of the 150 clinical cases (a total of 88,535 CMR images). Within each case, all the necessary tools to make the diagnosis are presented in exactly the same format as they are used every day at leading CMR clinical centers, including side-by-side movies, image magnification, single stepping, and even measurement tools (measurements require an internet connection). This format provides the student of CMR with the unprecedented opportunity to review

all of the data and attempt to reach their own conclusion and then reference an expert opinion simply by clicking on the "Case Discussion" Web link.

The cases comprising this Teaching File demonstrate the utility of CMR for the entire spectrum of cardiovascular pathology. Straightforward "bread-and-butter" cases are presented, along with more unusual entities. The first few cases are designed to introduce the reader to the display format and to the techniques used in CMR, including the mechanics and nuances of image acquisition. The cases that then follow can be sorted by category (congenital heart disease, cardiomyopathies, etc.) if desired, but are otherwise presented in a random format to allow readers to test themselves in interpreting "unknowns." In the initial presentation of the images, the history is withheld, but clicking the "history" button at the top of the page will reveal it.

Through this presentation of unknown cases, the reader can encounter the unfiltered "raw data" of real patient scans, can formulate their own opinion, and then can obtain immediate feedback by reading the discussion. In addition, references are attached to virtually every case. Since the cases are viewed using a standard web browser, if one is connected to the Internet, clicking on the associated links will take one directly to the abstract in PubMed. From there, one can do additional reading as desired.

The print portion of this project, which accompanies the DVD, is organized into two sections: Part I is an overview of CMR imaging, with an introduction to current techniques and applications. Part II is comprised of the Case Discussions that explain each case. Part III reviews scan planning and standard protocols. The printed material is thus available for offline reading, but is also reproduced on the DVD. This duplication is done to take advantage of the Web page format of the DVD, which allows the creation of links between related subjects. Since the DVD contents are displayed in a browser window, links from the Case Discussions to the Overview allow easy navigation from cases to didactic material and back to cases, facilitating the learning process (when using the DVD).

It is our hope that this assemblage of CMR cases will be helpful to those cardiologists and radiologists in training who are interested in learning CMR, particularly those training at facilities where they may not have an abundance of cases. We are biased of course, but we believe that CMR is one of the most exciting fields in medicine. We hope that the introduction to its various implementations as contained in this Teaching File will stimulate in the reader a broad and sustained interest.

John D. Grizzard, MD
Robert M. Judd, PhD
Raymond J. Kim, MD

Acknowledgments

This work would not have been possible without the hard work and expertise of a multitude of individuals. First among these is Tarik Koc, who did much of the laborious work of HTML coding involved in making the DVD an effective teaching tool, with links between sections and cases. Thanks also go to the many current and former cardiology fellows, radiology house staff, and technologists both at Duke and VCU who performed scans and suggested cases for inclusion.

We would also like to point out that the sections of this book relating to myocardial delayed contrast enhancement reflect knowledge gained from U.S. National Institutes of Health projects R01-HL064726 and R01-HL063268.

John D. Grizzard, MD
Robert M. Judd, PhD
Raymond J. Kim, MD

Contents

Preface vii
Acknowledgments ix
How to Use the DVD and the Book Together xiii

Part I Techniques and Applications

1 Overview 3
2 The Standard Cardiac Exam 17
3 Ischemic Heart Disease and Non-Ischemic Cardiomyopathies 25
4 Hemodynamic Assessment and Congenital Heart Disease 41
5 Pericardial Disease and Cardiac Masses 49
6 MR Angiography: General Principles 59
7 Body MRA 65
8 Peripheral MRA 75

Part II Cases 83

Part III Appendixes

A Acronyms 267
B Cardiac Scan Planning 269
C Cardiac Imaging Modules 275
D Suggested Protocols 279
Index 289

How to Use the DVD and the Book Together

As opposed to many book-DVD combinations, in the instance of this endeavor, the DVD is the "heart" of the project, while the printed material is supplementary. To get started, simply insert the DVD into your computer and navigate to and open the folder containing the Book. Then, click the "Getting_Started.html" icon and the Teaching File will load in a browser window. The reader will note that the home page for the project has a "window-frame" appearance wherein the navigation placemarks (Book, Cases, Training, etc.) are present along the left margin of the screen, while the central "pane" shows the case images, or the book text, etc. Selecting "Cases" will result in the display of a drop-down menu allowing choice "by number" of the cases in 20 case increments. However, the cases can also be sorted by category. Clicking on "The Book" will take one to the title page of the Book. Choosing the "Table of Contents" drop-down menu will take the reader to an interactive Table of Contents that has links to the various sections and chapters of the Book.

The Webpax® interface used for the presentation of the cases provides a user-friendly format for the display of cardiovascular images. This unique interface allows visualization of cardiac motion at the patient's native heart rate (assuming sufficient computer resources) as present during the scan. These images can be viewed using any standard web browser, although the authors' prefer Firefox® (http://www.mozilla.com/en-US/firefox/) since this browser appears to more faithfully follow W3C web standards. Multiple looping images can be viewed simultaneously, facilitating comparison of the various segments. Clicking on any given image will result in the image being magnified. In addition, a scroll bar will then become evident, which provides the reader the ability to rapidly move back and forth through the stack of images. If two or more "magnified" views are desired, one can open multiple browser windows, each with their own view. The thumbnail images are presented as animated GIFs, and right clicking on the image and "saving as" will allow one to save the image. Alternatively, if one has an Apple computer, one can simply drag the image and drop it onto the desktop or directly onto a PowerPoint slide. Many tools, including the ability to download the magnified views as AVI or animated GIF files, have been disabled for offline viewing, however, if an internet connection is available these tools will be available during online viewing. For AVI files, the reader can select the play speed or frame rate, but the default (for cine images) is the patient's native heart rate.

The majority of cases are displayed in a standardized format, wherein the short-axis cine views are presented in the top row, arranged from base to

apex as one proceeds from left to right. In the case of a stress / rest perfusion study, the stress images are presented in the first three or four images of the second row, and are arranged so that they are directly below the corresponding cine image acquired at the same location. The rest perfusion images are displayed in the third row, again at exactly the same image locations. Finally, the delayed-enhancement images (again spatially matched to the cine and perfusion images) are displayed in the fourth row. This arrangement facilitates the comparison of wall motion with stress and rest perfusion and viability. In cases performed without perfusion imaging, the display arrangement may demonstrate some variability, but the essential images necessary for diagnosis will be available.

Each case has an associated discussion that reviews the imaging findings and reveals the diagnosis. In addition, references are attached to virtually every case. Since the cases are viewed using a standard web browser, if one is connected to the Internet, clicking on the associated links will take one directly to the abstract in PubMed. From there, one can do additional reading as desired.

It is suggested that the reader initially attempt evaluation of the images alone, before turning to the discussion. It is our hope that the discussions will suggest to the reader a systematic approach to the evaluation of CMR images. The abundance of information presented in a typical CMR case can be overwhelming at times, and only through the application of a consistent reading format will one be assured of detecting all the important findings in a given case. In general, the approach used in the Teaching File follows this sequence: 1) LV–Cavity size, wall thickness, global and regional wall motion (using the 17-segment model). 2) RV–Cavity size, wall thickness, global and regional wall motion. 3) Valves–Mitral, aortic, tricuspid, pulmonic; evaluate for morphology and thickening, regurgitation, and stenosis. 4) Atria –Size, emptying, masses/ thrombi (left atrial appendage in particular). 5) Perfusion images (if performed)–Compare stress/rest images if both performed in order to exclude artifact. Evaluate for defects; compare to analogous regions on cine and delayed-enhancement images. 6) Delayed-enhancement imaging–Compare to perfusion and cine images at same spatial locations. If hyperenhancement is present, determine if it is in a CAD or Non-CAD pattern. Determine the transmural extent of hyperenhancement (infarction for patients with CAD) using the 17-segment model and a 5-point scale for each segment. Evaluate long-inversion-time images for thrombi. 7) Global overview–Evaluate pericardium for thickening, fluid; mediastinum and lungs for masses, etc.

MR angiographic images are also presented, and the utility of MRA for imaging a variety of vascular territories will be discussed. Because of the variety of body regions examined, it is difficult to suggest a single reading technique. A few caveats, however, are offered: 1) When possible, think physiologically when evaluating an MRA study, and not simply anatomically. For instance, looking for associated collaterals that would be expected in cases of chronic occlusion facilitates the correct characterization of an abrupt vessel-cutoff as being due to a stent artifact rather than an occlusion. 2) These studies encompass a lot of anatomy, and attention to extra-vascular structures is important to avoid missing significant pathology.

The Overview of Cardiovascular MR Imaging included with the Teaching File is not designed as a comprehensive textbook, but rather is intended to serve as a quick reference to the current techniques and principles used in everyday CMR imaging. It can be read prior to attempting to tackle the Teaching File cases, or may simply be referred to on an "as-needed" basis,

depending on one's experience and training. The scanning protocols used by the authors for a variety of indications are included in the Appendix, along with a glossary of acronyms to help the reader decode the "alphabet soup" of abbreviations found in CMR.

John D. Grizzard, MD
Robert M. Judd, PhD
Raymond J. Kim, MD

Part I
Techniques and Applications

1
Overview

Introduction
CMR Techniques
  Morphologic Imaging Using Dark-Blood Sequences
  Morphologic Imaging Using Bright-Blood Sequences
  Cine Imaging
  Perfusion Imaging
  Viability Imaging
  Flow-Sensitive Imaging Using Velocity-Encoded Sequences
  MR Angiography
  Parallel Imaging Acquisition Techniques
  Summary
CMR Safety
References

Introduction

Over the last several years, cardiovascular magnetic resonance (CMR) has undergone rapid evolution, and tremendous advances in pulse sequence design, scanner hardware, and coil technology have resulted in progressive expansion of the clinical applications.[1–4] In particular, new pulse sequences have leveraged the inherently superior soft tissue contrast provided by MR so that it now provides the reference standard for in vivo viability imaging.[5] Additionally, the pattern and distribution of scar as demonstrated by CMR often provides useful information regarding the specific etiology of various cardiac disorders.[6, 7] Similarly, for imaging cardiac structure and function, pulse sequence and hardware developments have resulted in improvement in image quality with simultaneous acceleration of image acquisitions, resulting in shorter but better examinations. Improved coil design now allows the use of parallel imaging technology, resulting in further reductions in acquisition times.[8, 9] These improvements have led to the recognition of CMR as the reference standard for the assessment of regional and global systolic function,[10, 11] the detection of myocardial infarction and viability,[12, 13] and the evaluation of pericardial disease and cardiac masses.[14, 15] In some centers, CMR is emerging as the test of choice for the detection of ischemic heart disease, as well as for the initial work-up of patients presenting with heart failure.[16, 17]

As CMR moves from a research tool into the clinical mainstream, there has been a gradual recognition of the need for standardized imaging protocols. This process is ongoing, but the Society of Cardiovascular Magnetic Resonance has formulated initial guidelines for imaging modules that can be combined as needed for a variety of

different examinations. The cases presented in the Teaching File in Part II were acquired using protocols similar to these guidelines, and our versions of these guidelines are listed in the appendix. This chapter provides a brief overview of the common techniques used in CMR. The subsequent chapters then outline the standard cardiac examination, discuss specific applications for the assessment of a variety of cardiac disorders, and provide some suggestions on how to optimally use this Teaching File. Several of the individual Teaching File cases will also review the techniques of image acquisition, and the parameters used for given sequences.

CMR Techniques

A unique characteristic of MR imaging is that a variety of information can be obtained simply by selecting different software sequences to probe the tissue characteristics of the organ in question. Multiple pulse sequences are available for cardiac MR imaging and can provide morphologic, cine, perfusion, viability, and velocity-encoded flow images. Also, certain image sequences may be utilized to produce cine images wherein multiple phases at the same slice location are obtained, or the same sequence may be run as a multislice acquisition where single phases at multiple locations are obtained. Although the physics underlying these pulse sequences are beyond the scope of this overview, a brief consideration of pulse sequences and the resulting images is presented to provide background for the Teaching File cases.

Morphologic Imaging Using Dark-Blood Sequences

This was the initial application of MR imaging for evaluating the heart. Initial implementations used spin-echo techniques, and subsequently fast spin-echo acquisitions were developed that resulted in decreased imaging time. For the most part, morphologic black blood imaging is now performed with single-shot double inversion fast spin-echo techniques (Double-IR FSE, and HASTE or half-Fourier acquisition turbo spin-echo). These result in still-frame images and are usually acquired in the standard orthogonal imaging planes (axial, sagittal, or coronal) (Figure 1.1) (Case 66, series 2 and 4). The TR is typically set at 90% of the R-R interval, and adjusted to null the signal from blood. The images are acquired at every other heartbeat, and are quite useful for rapid morphologic imaging. A fat-saturation prepulse can also be applied. The rapidity of acquisition is such that breath holding is not required. These produce excellent depiction of the overall myocardial structure, as well as the relationships of the great vessels. They also provide excellent depiction of the walls of the great vessels and myocardium.

Occasionally, segmented fast spin-echo images are acquired when higher spatial resolution and/or

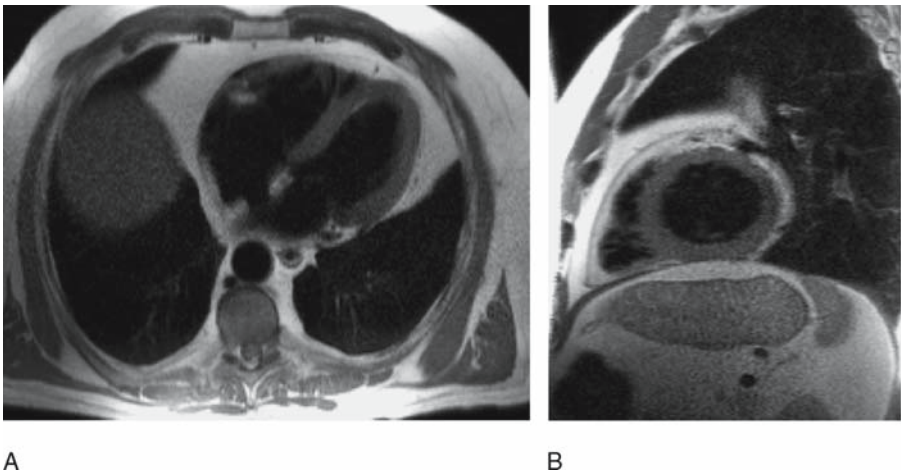

FIGURE 1.1. Axial **(A)** and sagittal **(B)** half-Fourier acquisition single-shot turbo spin-echo (HASTE) images

improved T1- or T2-weighting is desired, such as when characterizing cardiac masses. These acquisitions take approximately 7 to 10 seconds per image and require breath holding. They can be performed either with or without fat saturation.

Morphologic Imaging Using Bright-Blood Sequences

Bright blood imaging was usually performed with gradient-recalled echo pulse sequences, which resulted in bright intracavitary signal due to the inflow of moving blood. However, slow flow could result in poor depiction of the interface between the blood pool and myocardium.

Steady state free precession (SSFP) sequences have resulted in significant improvement in bright blood imaging. With these sequences, image contrast is not as dependent on inflow effects, but rather on the different physical characteristics of tissues. Specifically, signal intensity is dependent on the T2/T1 ratio of the tissue being imaged[18] (not including effects from prepulses), and this results in bright signal for intracavitary blood, and a relatively dark appearance for myocardium. Images can be rapidly acquired typically in less than 300–400 ms per image. These sequences do not require breath holding and are similar to HASTE sequences in that they are a form of single-shot imaging. For cardiovascular structures, one image is typically acquired each heartbeat (at the same cardiac phase), and a stack of 30 images can be acquired in approximately 30 seconds (Figure 1.2) (Case 66, series 3 and 5) SSFP sequences are very useful in the evaluation of disorders producing intraluminal abnormalities. For example, they can be used for the evaluation of aortic dissection and for localization of the pulmonary veins prior to MR angiography.

Cine Imaging

The same steady state free precession (SSFP) technique used to produce bright blood static images may be adapted for cine acquisition. In this instance, multiple images are obtained at a single slice location in rapid succession during different phases of the cardiac cycle and can be displayed as a continuous movie loop.[19, 20] Cine imaging allows evaluation of ventricular wall motion abnormalities, dynamic changes in wall thickness, and measurement of chamber sizes. It also allows assessment of valvular morphology and function (Figure 1.3) (Case 66, series 33).

The standard cine sequence is a segmented, retrospectively gated acquisition, in which the data is acquired throughout the cardiac cycle and is "time stamped" to allow assignment to the proper cardiac phase. The segmented acquisition indicates that data from several heart beats is combined to yield the image. As such, irregularities in

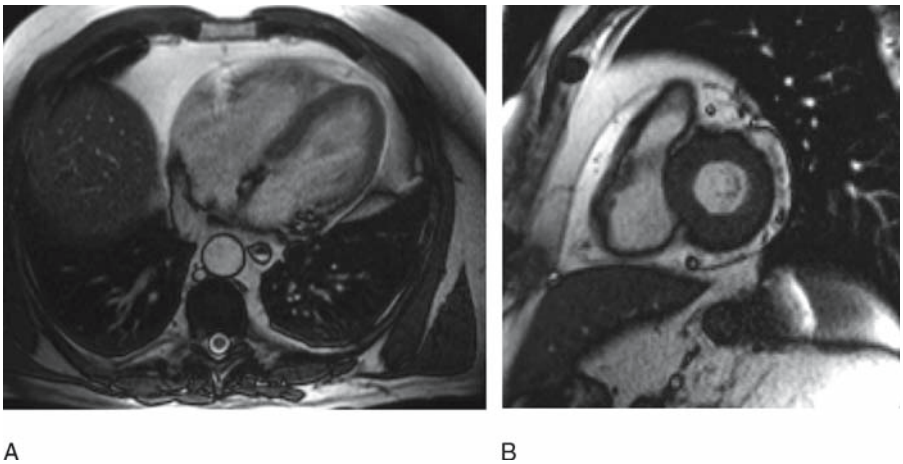

FIGURE 1.2. Axial **(A)** and sagittal **(B)** steady-state free precession (SSFP) images

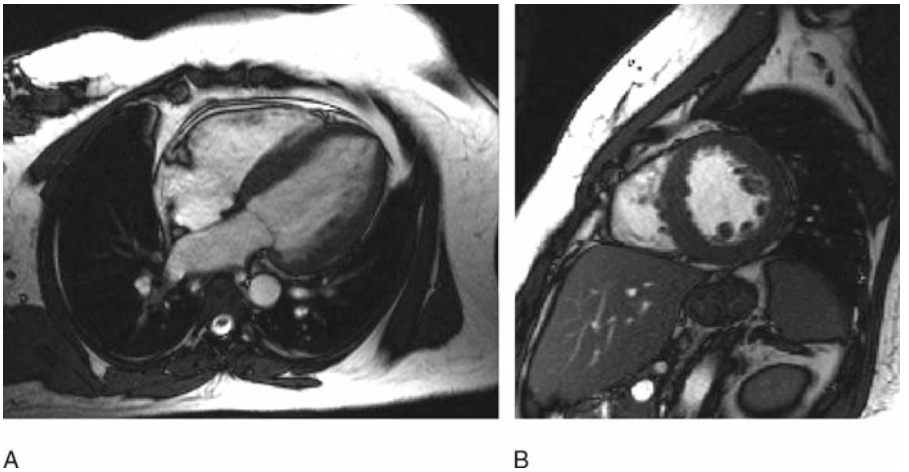

FIGURE 1.3. Four-chamber **(A)** and short-axis **(B)** cine images using SSFP

the patient's heart rate and rhythm may degrade image quality.

In cases of arrhythmia, prospectively triggered acquisitions may be helpful. Since changes in heart rate predominately affect the length of diastole rather than systole, this strategy by beginning with the R wave and acquiring a predetermined length of time (usually up to early or mid diastole), can remove some of the artifacts that result from irregular cycle lengths. Unfortunately, prospectively triggered acquisitions often result in the loss of the terminal phase of diastole, and correspondingly, measurements of ventricular ejection fraction and chamber volumes from these acquisitions may be slightly imprecise. If gating is unsuccessful, or the arrhythmia is severe, or the patient cannot breath-hold adequately, real-time cine acquisitions may be necessary. These acquisitions also employ steady state free precession sequences, albeit in a single-shot rather then segmented fashion. Although these acquisitions have lower spatial and temporal resolution, they may provide sufficient information for diagnosis. In addition, real-time cine acquisitions can be helpful in the detection of dynamic processes, as they can be acquired during inspiratory and expiratory maneuvers.

Perfusion Imaging

These sequences are designed to demonstrate contrast media passage through the myocardium in a manner that reliably reflects myocardial blood flow. It is desirable to have multiple slices during each heartbeat in order to ensure sufficient ventricular coverage, with high temporal resolution.[12, 21, 22] The sequences used by different manufacturers differ, but the general strategy is to utilize a saturation prepulse to accentuate T1-weighting, and thus accurately depict the passage of a T1 shortening contrast agent such as gadolinium.[23] These sequences are very gradient intensive, such that only high performance magnets are capable of executing these sequences with adequate temporal and spatial resolution. In the implementation used throughout this teaching file, a saturation recovery gradient-recalled echo sequence has been used. Each slice takes approximately 160 ms to acquire (120 ms for image acquisition, 40 ms to allow partial recovery of magnetization) and therefore 4 slices require a total of 640 ms. Given that the R-R interval is approximately 640 ms when the heart rate is 94 beats per minute, 4 slices can be obtained in most patients unless tachycardia is present.

Perfusion imaging is most often used for the detection of obstructive coronary artery disease, where it is performed with pharmacological vasodilation (e.g. adenosine). The underlying principle is similar to that in nuclear perfusion imaging, where a vasodilator is used to accentuate regional differences in myocardial blood flow. During adenosine infusion, myocardial blood flow increases approximately 4-fold downstream of

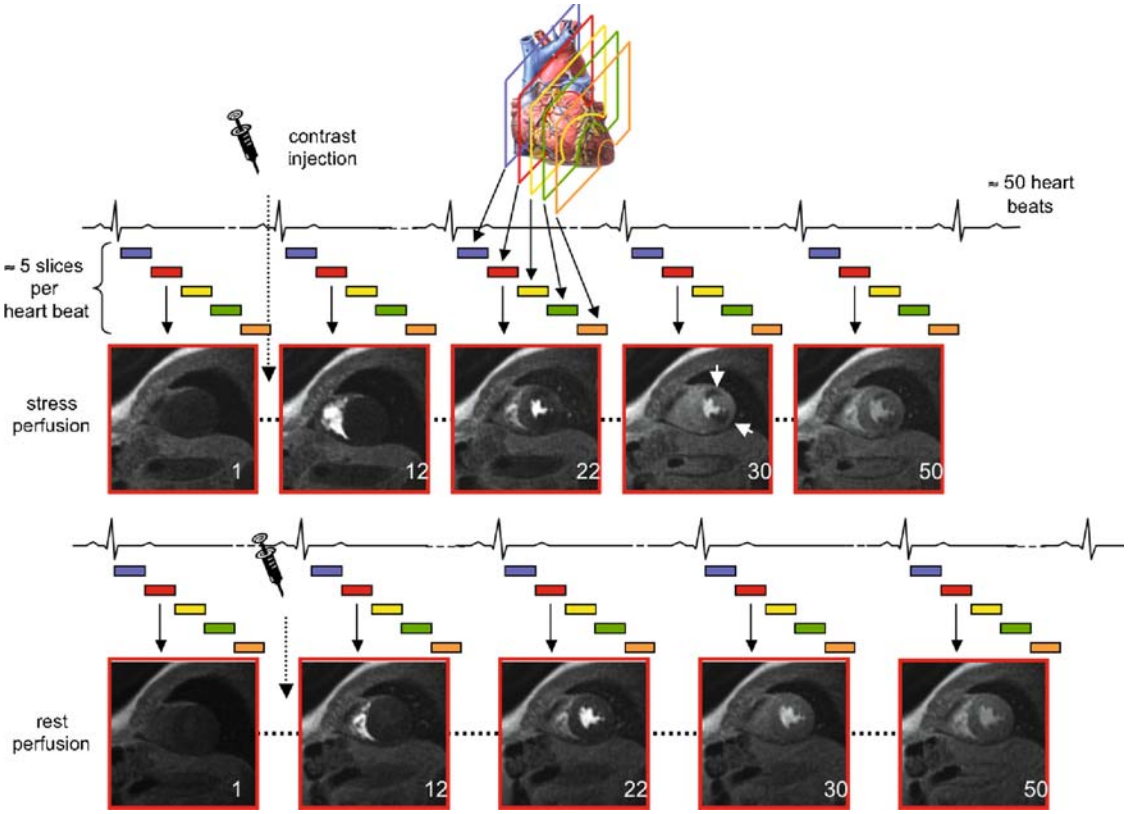

FIGURE 1.4. First-pass perfusion MR image acquisition. Images are acquired serially at multiple slice locations (usually four to five short-axis views for left ventricular coverage) every heartbeat to depict the passage of a compact contrast bolus as it transits the heart. Example images of one slice location are shown at several representative timepoints: before arrival of contrast (frame 1); contrast in RV cavity (frame 12); contrast in LV cavity (frame 22); peak contrast in LV myocardium (frame 30), showing normal perfusion in the septum *(open arrowhead)* and abnormal perfusion in both the anterior and inferolateral walls *(solid arrowheads)*; and the contrast wash-out phase (frame 50)

normal coronary arteries, but does not increase (or increases minimally) downstream of severely diseased arteries because the arteriolar beds are already maximally vasodilated (Figure 1.4) (Case 25, series 21.3). However, there are some differences as compared with nuclear perfusion imaging, MR perfusion imaging is a first pass imaging study that directly images the passage of contrast, and therefore is performed using an abbreviated adenosine protocol (~3 minutes). Also, MR perfusion imaging has higher spatial resolution than nuclear techniques, and can depict a perfusion defect that is only subendocardial. MR perfusion imaging has the additional advantage of providing a more linear depiction of myocardial blood flow in response to vasodilatation, without the plateau phenomenon seen with nuclear agents.[24] Although research studies often emphasize analysis of the upslope curves and other complex post-processing of the perfusion data, recent reports using visual analysis demonstrated comparable sensitivity and specificity.[25, 26] This is the approach used throughout this Teaching File.

Perfusion imaging can also be used in the evaluation of suspected intracardiac shunts, as well as in the characterization of cardiac masses.

Viability Imaging

It is important to note that normal myocardium as well as infarcted and scarred myocardium will demonstrate contrast enhancement. However, they

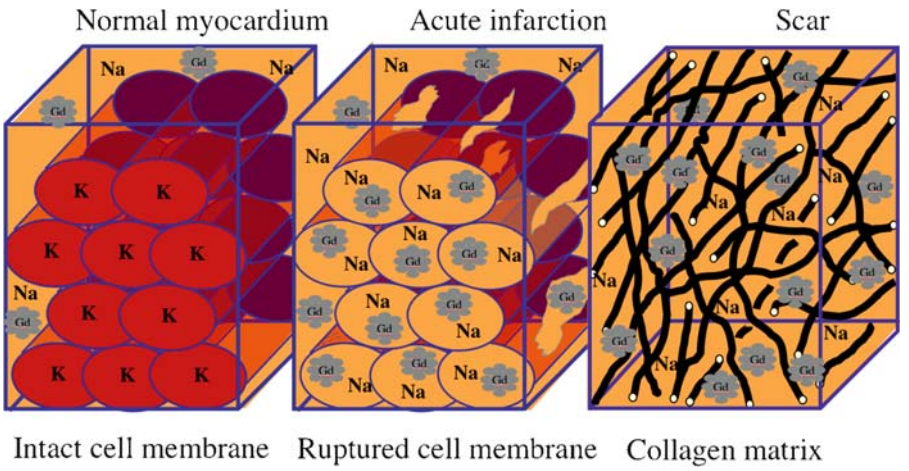

FIGURE 1.5. The volume of distribution for gadolinium is increased in both acute and chronic infarcts. (From Shah et al, Myocardial Viability. In: Edelman et al, eds. *Clinical Magnetic Resonance Imaging (3rd ed.)*. New York, NY: Elsevier; 2006)

have different contrast kinetics in that contrast will washout of normal myocardium at a much more rapid rate than it will from infarcted or scarred myocardium.[27] In addition, areas of infarction, whether acute or chronic, will have a larger relative amount of extracellular space and therefore a greater volume of distribution for gadolinium contrast than will normal myocardium (Figure 1.5) Accordingly, areas of prior infarction will have higher concentrations of contrast on delayed images (5 to 10 minutes after intravenous administration).[28] The delayed-enhancement sequences used for infarct detection are designed to maximize the differential signal intensity between normal myocardium and infarcted myocardium.[29]

The standard delayed-enhancement imaging sequence incorporates a segmented gradient echo read-out and an inversion prepulse to produce heavy T1-weighting.[30] The inversion pulse serves to flip the magnetization 180 degrees. The recovery of magnetization back to baseline by areas that have a higher gadolinium concentration will be more rapid (as they have a lower T1 value) than those with a lower concentration of gadolinium such as normal myocardium. Therefore, the increased concentration of gadolinium in an area of scar will be reflected by more rapid return above the zero-crossing line and back to baseline longitudinal magnetization (Figure 1.6) The time after the inversion pulse at which normal myocardium is at the zero-crossing line will result in maximum suppression of signal from normal myocardium (the myocardium is said to be "nulled"), and will result in maximum conspicuity of the area of infarction. At this time point, infarcted regions will be well above the zero-crossing line and therefore, will appear bright on these images (Figure 1.7) (Case 3, series 50).

The standard delayed-enhancement sequences are segmented acquisitions, acquired at every other heartbeat in order to allow normal myocardial regions to recover longitudinal magnetization before the next inversion pulse is applied. Therefore, they are constructed from the data of multiple heartbeats. They typically take approximately 8 to 12 seconds to acquire. For patients with significant arrhythmia, or difficulty with breath holding, single-shot delayed-enhancement images using an SSFP inversion recovery sequence can provide a reasonable alternative in a fraction of the imaging time.[31, 32] These images are slightly lower in contrast to noise ratio, and have a mildly reduced sensitivity for the detection of infarction, but provide a satisfactory option in these circumstances (Case 3, series 30).

Single-shot delayed-enhancement imaging may also be obtained with a long inversion time (550 to 600 ms). These are quite useful in the detection of thrombi.[15] On these images, thrombi will appear dark in contrast to normal myocardium and infarcted myocardium, which will be grey and bright in image intensity, respectively (Figure 1.8) (Case 11, series 39).

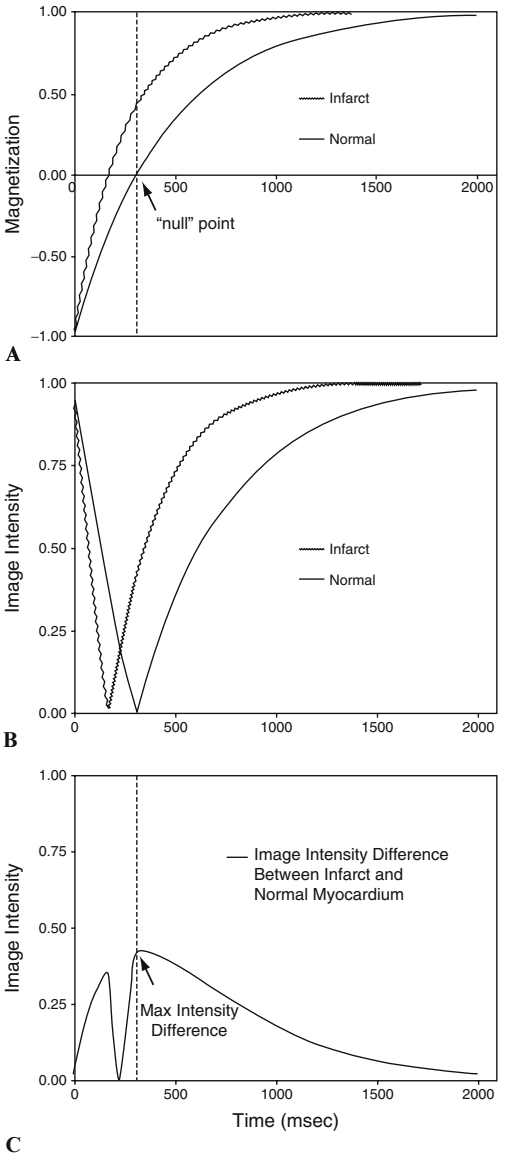

FIGURE 1.6. **(A)** Inversion recovery curves of normal and infarcted myocardium assuming T1 of normal myocardium is 450 msec and infarcted myocardium is 250 msec. The time at which the magnetization of normal myocardium reaches the zero crossing is defined as the inversion time to "null" normal myocardium. **(B)** Image intensities resulting from an inversion prepulse with various inversion delay times. Note that image intensities correspond to the magnitude of the magnetization vector and cannot be negative. **(C)** Difference in image intensities between infarcted and normal myocardium as a function of inversion time. The optimal inversion time is when the maximum intensity difference occurs. (From *J Cardiovasc Magn Reson* 2003;5:505–514, with permission)

Although predominately associated with the assessment of myocardial infarction and viability, the same delayed-enhancement sequences can also be helpful in a variety of other circumstances, such as the detection of viral myocarditis, identification of cardiac involvement by sarcoidosis, and the differentiation of ischemic from non-ischemic cardiomyopathy.[6, 33, 34]

Flow-Sensitive Imaging Using Velocity-Encoded Sequences

In this form of imaging, velocity-encoding phase shifts result from the sequential application of bipolar magnetic field gradients, which are composed of two lobes with opposite polarities. These opposed gradients will produce a phase shift with the first pulse that will be reversed by the second pulse. Therefore, stationary spins will acquire equal and opposite phases in the two gradients, and will have no net phase at the end of the sequence. However, flowing spins will acquire a net phase change, which will be dependent on their velocity in the direction of the flow-encoding gradients.[35–37] Gradients can be varied in amplitude or duration to sensitize the pulse sequence to fast or slow flow. The maximum velocity encoded by the sequence is termed the Venc and is selected by the operator.

Aliasing occurs when the maximum velocity sampled exceeds the upper limit imposed by the chosen Venc, resulting in apparent velocity reversal. To avoid aliasing the velocity threshold must be correctly selected (Case 20, series 43). Aliasing results in artifactual reduction of the measured flow, in direct proportion to the extent of aliasing, and therefore accurate flow measurements require its recognition. It is recognized in the velocity images where the voxels of assumed peak velocities have an inverted signal intensity compared with that of surrounding voxels.

The optimal Venc should just exceed the anticipated velocities to be measured. Setting the Venc too high will lead to increased noise or inaccuracy in the velocity or flow measurement. With sequences currently available, phase-contrast measurement can be performed in a breath hold using retrospective cardiac gating. Both the magnitude and phase images are often reviewed (Figure 1.9) (Case 20, series 46 and 47).

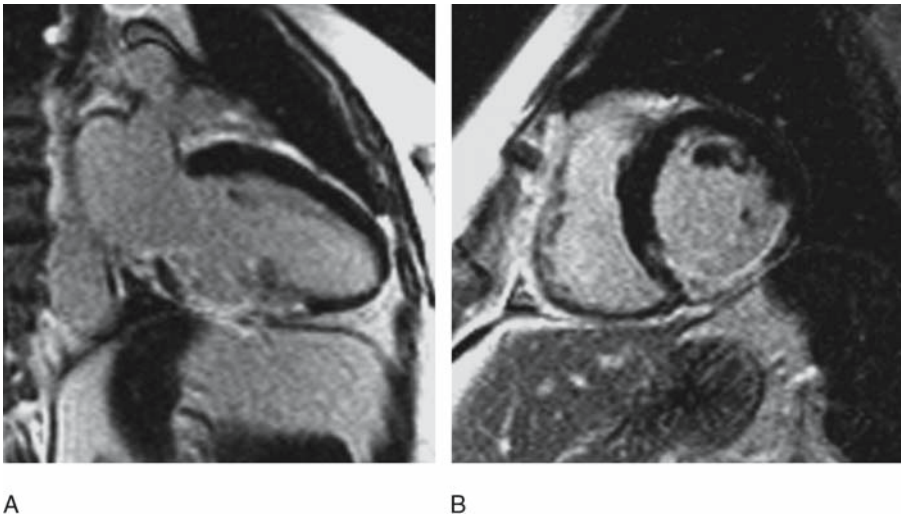

FIGURE 1.7. Inversion recovery delayed-enhancement images demonstrate an infarct in the right coronary artery territory

These sequences are typically used in two situations—quantification of gradients across stenotic valves, and for measurement of blood flow. The peak gradient across a stenotic valve can be calculated using the Bernouilli equation, $\Delta P = 4\ V^2$ where velocity V is in meters per second, and the gradient is given in mm Hg. On most scanners, the velocities are given in cm/sec, and must be converted to m/sec for the calculation. Flow is simply the sum of the velocities through a given area over time. These measurements are typically performed during post-processing using a dedicated workstation.

MR Angiography

Although previously noncontrast time-of-flight sequences were used, currently MR angiography

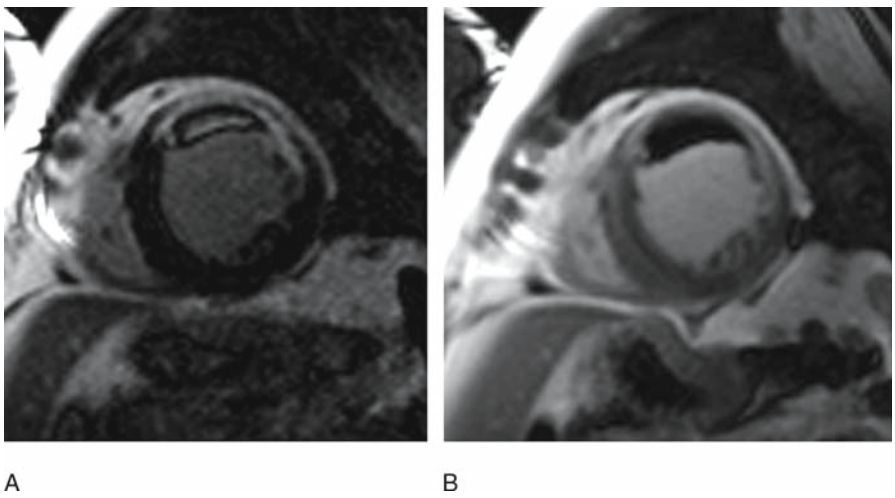

FIGURE 1.8. Short-axis single-shot inversion recovery delayed-enhancement images obtained with inversion times of 300 ms **(A)**, and 600 ms **(B)**. Note that the mural thrombus adherent to an anterior wall infarction appears high in signal intensity on the image where myocardium is nulled as it is well below the zero-crossing line. It is low in signal on the image with a long inversion time

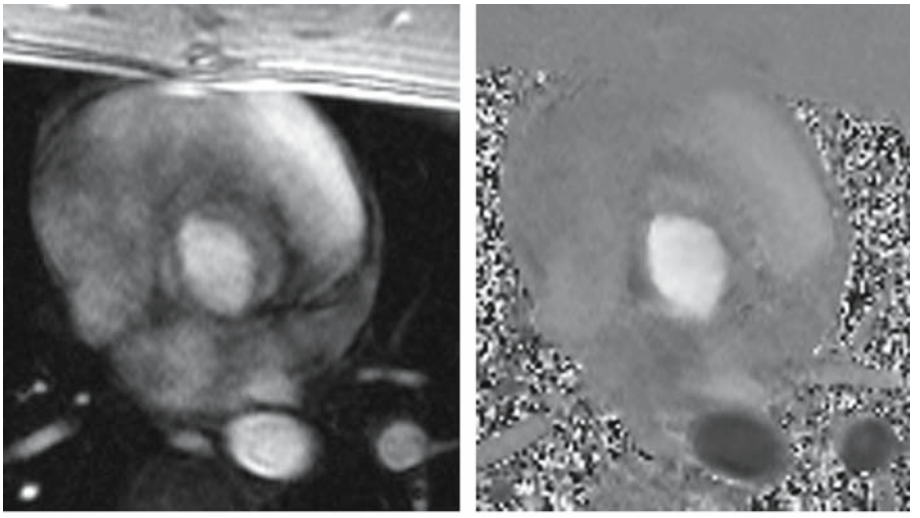

FIGURE 1.9. Magnitude **(A)** and phase **(B)** images from a velocity-encoded study of a bicuspid aortic valve

is most often performed using thin section T1-weighted spoiled gradient-echo image acquisitions during the arterial passage of intravenously administered contrast.[38–43] Synchronization of image acquisition with the arterial passage of contrast is most often performed by using fluoroscopic monitoring of the contrast passage, with scan initiation triggered after visualization in the appropriate region (Case 15, series 40). Alternatively, a timing bolus technique may be used.[44] In this technique, a small (2 cc) bolus of contrast is administered and sequential images are obtained at a predetermined location at a rate of one per second. The arrival time of the contrast bolus is then used to calculate the appropriate time for scan triggering (Case 16, series 12).

Multiple thin slices are obtained in a 3-D volumetric technique, and are then assembled into maximum intensity projection images, as well as volume rendered images. Multi-planar review of the obtained images is also performed, in order to visualize the vessels in cross-section and to evaluate the vessel walls. This review is facilitated by the acquisition of the image data in isotropic voxels, which allow reformation into any desired plane without image degradation. The plane of imaging is freely selectable with MR angiography, but by convention, thoracic studies are usually performed in either the axial or sagittal plane. An oblique sagittal plane that provides a "candy cane" view of the thoracic aorta may be used to minimize breath hold time by reducing the thickness of the imaging slab. Abdominal, pelvic, and extremity studies are usually obtained in the coronal plane (Figure 1.10) (Case 16, series 13).

The in-plane image resolution, the slice thickness, and the volume of coverage are all freely

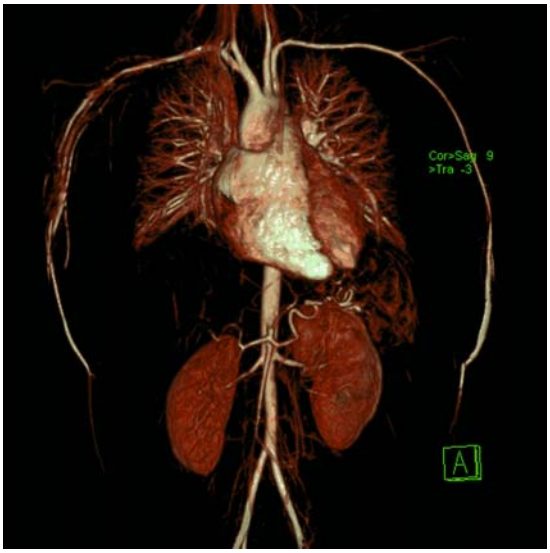

FIGURE 1.10. Volume-rendered image from a contrast-enhanced MR angiogram

selectable parameters. Increasing in-plane resolution will increase imaging time, as will diminishing slice thickness for a given volume of acquisition. Therefore, in situations where breath holding is required such as in chest and abdomen MR angiography, the duration of the acquisition becomes the limiting factor. A breath-hold exceeding 25 seconds becomes problematic for most patients, and imaging should generally be completed within this time frame. In circumstances where cardiac motion is likely to result in image degradation, such as imaging of the aortic root, the sequences can be acquired with electrocardiographic gating. In this situation, imaging can be timed to when cardiac motion is minimal (i.e. diastole), however, since data is acquired only during a portion of the cardiac cycle, voxel size is usually increased to maintain the same breath hold duration.

The use of MR angiography has been well validated in a variety of vascular regions, most notably for evaluation of renal artery stenosis where it compares favorably with digital subtraction angiography.[40, 45] It is also been well accepted for abdominal, pelvic, and lower extremity runoff imaging for comprehensive multistation evaluation of the peripheral vasculature in patients likely to require revascularization.[46–48] It has advantages over conventional catheter and CT angiography in that no radiation or potentially nephrotoxic contrast is required. The examination can be performed in 30 minutes. No arterial puncture is required.

Parallel Imaging Acquisition Techniques

Although the different scanner manufacturers have their own proprietary implementations, all support parallel imaging techniques. These allow a reduction in image acquisition time, or improvement in spatial resolution with the same imaging time, but at a cost of mildly reduced signal-to-noise. This reduction is roughly proportional to the square root of the acceleration factor used, so that at the usual implementation of an acceleration factor of 2, the resultant signal-to-noise of the accelerated image is approximately 70% of the nonaccelerated image.[8, 49] These techniques can be applied to all of the imaging sequences previously described, and are most helpful in cardiac imaging.

Summary

Cardiac MR imaging has made tremendous progress in the past decade. Multiple different sequences are available and provide the ability to interrogate cardiac structure, function, and viability with unparalleled precision. These sequences individually and in combination provide a diverse palette from which to choose. Recommendations for specific choices that will comprise a “Standard Cardiac Exam” follow in the next chapter.

CMR Safety

The CMR imaging environment has the potential to pose serious risks to patients and facility staff in several ways. Injuries can result from the static magnetic field (projectile impact injuries), very rapid gradient-field switching (induction of electric currents leading to peripheral nerve stimulation), RF-energy deposition (heating of the imaged portion of the body), and acoustic noise. The institution of policies that strictly limit access to the magnet room minimizes the risks of projectile injuries from the static magnetic field. For instance, patients are extensively screened prior to imaging, and all facility personnel undergo dedicated training in MR safety. The use of *MR-safe* or compatible equipment (stethoscopes, wheelchairs, gurneys, oxygen tanks, infusion pumps, monitors, etc.) with clear labeling of such in the scanner area reduces this risk further. The Food and Drug Administration (FDA) has placed limits on the rate of change of gradient magnetic fields (e.g. the slew rate) and the amount of RF energy (e.g., specific absorption rate [SAR]) that can be transmitted to patients. All scanners monitor the slew rate and calculate the SAR to help prevent nerve stimulation and heating. Acoustic noise of 100 dB or more are generated from the vibration or motion of the gradient coils during image acquisition. The use of protective hearing devices, such as headphones or earplugs, reduces noise to levels that do not result in hearing impairment or patient discomfort. In practice, continuous communication with the patient throughout the examination is important for patent comfort and safety.

Patients with medical devices or implants can face additional potential hazards, including device

heating, movement, or malfunction. For example, ferromagnetic aneurysm clips or electronic medical devices (e.g., neural stimulators, insulin pumps) are strict contraindications to MRI. However, there is a specific subset of patients with a metallic implants or devices that can safely undergo MRI. A comprehensive list of devices and implants that are compatible with undergoing MRI scanning can be found elsewhere.[50,51] Regarding cardiac devices, it is important to note that prosthetic valves and coronary artery stents are now considered safe for MRI scanning.[50–52] Indeed, recently, the FDA approved the use of MRI immediately after the implantation of paclitaxel and sirolimus drug-eluting stents. At most institutions, MRI scans are not performed in patients with implanted pacemakers or defibrillators because of the potential risk of device malfunction, excessive device or lead heating, or induction of currents within the leads. Recently, however, a few preliminary reports have emerged, suggesting that MRI can be possible in patients with modern pacemakers and defibrillators in whom the benefits are deemed greater than the risks.[53–55] In patients in whom devices have been extracted, but with the leads remaining (permanent or temporary transvenous), MRI is contraindicated as the risk of heating or induction of currents can be higher.

Recently, in several small case series, it has been reported that a small subset of patients with end-stage renal disease, receiving gadolinium contrast, may be at risk for developing nephrogenic systemic fibrosis (NSF)[56]. NSF is characterized by an increased tissue deposition of collagen, often resulting in thickening and tightening of the skin and predominantly involving the distal extremities. Additionally, fibrosis may affect other organs, including skeletal muscles, lungs, pulmonary vasculature, heart, and diaphragm. Although a definitive causal link with gadolinium contrast agents has yet to be established, gadolinium contrasts agents should be utilized cautiously (and alternative tests considered) in patients with severe renal disease, particularly those undergoing peritoneal dialysis or hemodialysis, or with acute renal failure. A policy statement regarding the use of gadolinium contrast agents in the setting of renal disease has been published by the American College of Radiology.[56]

References

1. Fuster V, Kim RJ. Frontiers in cardiovascular magnetic resonance. Circulation. 2005;112(1):135–144.
2. Edelman RR. Contrast-enhanced MR imaging of the heart: overview of the literature. Radiology. 2004;232(3):653–668.
3. Lima JA, Desai MY. Cardiovascular magnetic resonance imaging: current and emerging applications. J Am Coll Cardiol. 2004;44(6):1164–1171.
4. Finn JP, Nael K, Deshpande V, Ratib O, Laub G. Cardiac MR imaging: state of the technology. Radiology. 2006;241(2):338–354.
5. Elliott MD, Kim RJ. Late gadolinium cardiovascular magnetic resonance in the assessment of myocardial viability. Coron Artery Dis. 2005;16(6):365–372.
6. Mahrholdt H, Wagner A, Judd RM, Sechtem U, Kim RJ. Delayed enhancement cardiovascular magnetic resonance assessment of non-ischaemic cardiomyopathies. Eur Heart J. 2005;26(15):1461–1474.
7. Isbell DC, Kramer CM. The evolving role of cardiovascular magnetic resonance imaging in nonischemic cardiomyopathy. Semin Ultrasound CT MR 2006; 27(1):20–31.
8. Glockner JF, Hu HH, Stanley DW, Angelos L, King K. Parallel MR imaging: a user's guide. Radiographics. 2005;25(5):1279–1297.
9. Niendorf T, Sodickson DK. Parallel imaging in cardiovascular MRI: methods and applications. NMR Biomed. 2006;19(3):325–341.
10. Bellenger NG, Burgess MI, Ray SG, et al. Comparison of left ventricular ejection fraction and volumes in heart failure by echocardiography, radionuclide ventriculography and cardiovascular magnetic resonance; are they interchangeable? Eur Heart J. 2000;21(16):1387–1396.
11. Bellenger NG, Grothues F, Smith GC, Pennell DJ. Quantification of right and left ventricular function by cardiovascular magnetic resonance. Herz. 2000;25(4):392–399.
12. Wagner A, Mahrholdt H, Sechtem U, Kim RJ, Judd RM. MR imaging of myocardial perfusion and viability. Magn Reson Imaging Clin N Am. 2003;11(1):49–66.
13. Wagner A, Mahrholdt H, Holly TA, et al. Contrast-enhanced MRI and routine single photon emission computed tomography (SPECT) perfusion imaging for detection of subendocardial myocardial infarcts: an imaging study. Lancet. 2003;361(9355):374–379.
14. Francone M, Dymarkowski S, Kalantzi M, Bogaert J. Magnetic resonance imaging in the evaluation of the pericardium. A pictorial essay. Radiol Med (Torino). 2005;109(1–2):64–74; quiz 75–66.
15. Grizzard JD, Ang GB. Magnetic resonance imaging of pericardial disease and cardiac masses. Cardiol Clin. 2007;25(1):111–140.

16. Dembo LG, Shifrin RY, Wolff SD. MR imaging in ischemic heart disease. Radiol Clin North Am. 2004;42(3):651–673, vii.
17. Rajappan K, Bellenger NG, Anderson L, Pennell DJ. The role of cardiovascular magnetic resonance in heart failure. Eur J Heart Fail. 2000;2(3):241–252.
18. Reeder SB, Herzka DA, McVeigh ER. Signal-to-noise ratio behavior of steady-state free precession. Magn Reson Med. 2004;52(1):123–130.
19. Fuchs F, Laub G, Othomo K. TrueFISP–technical considerations and cardiovascular applications. Eur J Radiol. 2003;46(1):28–32.
20. Pereles FS, Kapoor V, Carr JC, et al. Usefulness of segmented trueFISP cardiac pulse sequence in evaluation of congenital and acquired adult cardiac abnormalities. AJR Am J Roentgenol. 2001;177(5):1155–1160.
21. Wu KC. Myocardial perfusion imaging by magnetic resonance imaging. Curr Cardiol Rep. 2003;5(1): 63–68.
22. Schwitter J. Myocardial perfusion imaging by cardiac magnetic resonance. J Nucl Cardiol. 2006;13(6): 841–854.
23. Slavin GS, Wolff SD, Gupta SN, Foo TK. First-pass myocardial perfusion MR imaging with interleaved notched saturation: feasibility study. Radiology. 2001;219(1):258–263.
24. Lee DC, Simonetti OP, Harris KR, et al. Magnetic resonance versus radionuclide pharmacological stress perfusion imaging for flow-limiting stenoses of varying severity. Circulation. 2004;110(1):58–65.
25. Klem I, Heitner JF, Shah DJ, et al. Improved detection of coronary artery disease by stress perfusion cardiovascular magnetic resonance with the use of delayed enhancement infarction imaging. J Am Coll Cardiol. 18 2006;47(8):1630–1638.
26. Cury RC, Cattani CA, Gabure LA, et al. Diagnostic performance of stress perfusion and delayed-enhancement MR imaging in patients with coronary artery disease. Radiology. 2006;240(1):39–45.
27. Kim RJ, Fieno DS, Parrish TB, et al. Relationship of MRI delayed contrast enhancement to irreversible injury, infarct age, and contractile function. Circulation. 1999;100(19):1992–2002.
28. Rehwald WG, Fieno DS, Chen EL, Kim RJ, Judd RM. Myocardial magnetic resonance imaging contrast agent concentrations after reversible and irreversible ischemic injury. Circulation. 2002;105(2):224–229.
29. Fieno DS, Kim RJ, Chen EL, Lomasney JW, Klocke FJ, Judd RM. Contrast-enhanced magnetic resonance imaging of myocardium at risk: distinction between reversible and irreversible injury throughout infarct healing. J Am Coll Cardiol. 2000;36(6): 1985–1991.
30. Simonetti OP, Kim RJ, Fieno DS, et al. An improved MR imaging technique for the visualization of myocardial infarction. Radiology. 2001;218(1):215–223.
31. Sievers B, Elliott MD, Hurwitz LM, et al. Rapid detection of myocardial infarction by subsecond, free-breathing delayed contrast-enhancement cardiovascular magnetic resonance. Circulation. 2007;115(2):236–244.
32. Huber A, Schoenberg SO, Spannagl B, et al. Single-shot inversion recovery TrueFISP for assessment of myocardial infarction. AJR Am J Roentgenol. 2006;186(3):627–633.
33. Mahrholdt H, Goedecke C, Wagner A, et al. Cardiovascular magnetic resonance assessment of human myocarditis: a comparison to histology and molecular pathology. Circulation. 2004;109(10):1250–1258.
34. Sechtem U, Mahrholdt H, Hager S, Vogelsberg H. New non-invasive approaches for the diagnosis of cardiomyopathy: magnetic resonance imaging. Ernst Schering Res Found Workshop. 2006(55):261–285.
35. Glockner JF, Johnston DL, McGee KP. Evaluation of cardiac valvular disease with MR imaging: qualitative and quantitative techniques. Radiographics. 2003;23(1):e9.
36. Lotz J, Meier C, Leppert A, Galanski M. Cardiovascular flow measurement with phase-contrast MR imaging: basic facts and implementation. Radiographics. May-Jun 2002;22(3):651–671.
37. Buonocore MH, Bogren H. Factors influencing the accuracy and precision of velocity-encoded phase imaging. Magn Reson Med. 1992;26(1):141–154.
38. Edelman RR. MR angiography: present and future. AJR Am J Roentgenol. Jul 1993;161(1):1–11.
39. Kramer U, Nael K, Laub G, et al. High-resolution magnetic resonance angiography of the renal arteries using parallel imaging acquisition techniques at 3.0 T: initial experience. Invest Radiol. 2006;41(2):125–132.
40. Zhang H, Prince MR. Renal MR angiography. Magn Reson Imaging Clin N Am. 2004;12(3):487–503, vi.
41. Krinsky GA, Rofsky NM, DeCorato DR, et al. Thoracic aorta: comparison of gadolinium-enhanced three-dimensional MR angiography with conventional MR imaging. Radiology. 1997;202(1):183–193.
42. Leung DA, McKinnon GC, Davis CP, Pfammatter T, Krestin GP, Debatin JF. Breath-hold, contrast-enhanced, three-dimensional MR angiography. Radiology. 1996;200(2):569–571.
43. Finn JP. MR angiography in the abdomen. Magn Reson Imaging Clin N Am. 1995;3(1):13–21.
44. Hany TF, McKinnon GC, Leung DA, Pfammatter T, Debatin JF. Optimization of contrast timing for breath-hold three-dimensional MR angiography. J Magn Reson Imaging.2007;3:551–556.

45. Leung DA, Hany TF, Debatin JF. Three-dimensional contrast-enhanced magnetic resonance angiography of the abdominal arterial system. Cardiovasc Intervent Radiol. 1998;21(1):1–10.
46. Hany TF, Carroll TJ, Omary RA, et al. Aorta and runoff vessels: single-injection MR angiography with automated table movement compared with multiinjection time-resolved MR angiography–initial results. Radiology. 2001;221(1):266–272.
47. Ruehm SG, Hany TF, Pfammatter T, Schneider E, Ladd M, Debatin JF. Pelvic and lower extremity arterial imaging: diagnostic performance of three-dimensional contrast-enhanced MR angiography. AJR Am J Roentgenol. Apr 2000;174(4):1127–1135.
48. Kreitner KF, Kalden P, Neufang A, et al. Diabetes and peripheral arterial occlusive disease: prospective comparison of contrast-enhanced three-dimensional MR angiography with conventional digital subtr-action angiography. AJR Am J Roentgenol. Jan 2000;174(1):171–179.
49. Wintersperger BJ, Nikolaou K, Dietrich O, et al. Single breath-hold real-time cine MR imaging: improved temporal resolution using generalized autocalibrating partially parallel acquisition (GRAPPA) algorithm. Eur Radiol. Aug 2003;13(8):1931–1936.
50. Shellock FG, Kanal E. Magnetic Resonance: Bioeffects, Safety, and Patient Management. New York: Raven Press; 1994.
51. Shellock FG. Reference Manual for Magnetic Resonance Safety, Implants, and Devices. 2006 ed. Los Angeles, CA: Biomedical Research Publishing Group; 2006.145.
52. Patel MR, Albert TS, Kandzari DE, et al. Acute myocardial infarction: safety of cardiac MR imaging after percutaneous revascularization with stents. Radiology. 2006;240:674–680.
53. Roguin A, Zviman MM, Meininger GR, et al. Modern pacemaker and implantable cardioverter/defibrillator systems can be magnetic resonance imaging safe: in vitro and in vivo assessment of safety and function at 1.5 T. Circulation. 2004;110:475–482.
54. Roguin A, Donahue JK, Bomma CS, et al. Cardiac magnetic resonance imaging in a patient with implantable cardioverter-defibrillator. Pacing Clin Electrophysiol. 2005;28:336–338.
55. Nazarian S, Roguin A, Zviman MM, et al. Clinical utility and safety of a protocol for noncardiac and cardiac magnetic resonance imaging of patients with permanent pacemakers and implantable-cardioverter defibrillators at 1.5 tesla. Circulation. 2006;114:1277–1284.
56. Kanal E, Barkovich AJ, Bell C, et al. ACR Guidance Document for Safe MR practices: 2007. Am J Radiology. 2007;188:1–27.

2
The Standard Cardiac Exam

Core Components and Common Modifications
Interpretation and Reporting
General Applications – Quantitative Evaluation of Structure and Function
References

Core Components and Common Modifications

Chapter 1 explained that an extensive array of MR sequences are available for cardiac imaging. Each of these sequences can provide complementary information, often of incremental value. The desire for the most comprehensive imaging possible, however, must be counterbalanced with the recognition of the limited time available for scanning based on patient tolerance and scanner availability. The judicious use of resources mandates that the essential information be acquired in the least amount of time possible.

At a minimum, a standard cardiac MR examination should provide a comprehensive evaluation of the structure and function of the heart. Additionally, in the vast majority of patients, myocardial tissue characterization—with an assessment of infarction, scarring, and viability—provides substantial clinical value at minimal time cost.

In light of the above, our standard cardiac examination includes the following:

1. **Localizer scout images.** (To localize the heart within the chest and determine the appropriate cardiac imaging planes).
2. **Cine images in the short-axis plane from above the mitral valve through the cardiac apex, as well as in the standard orthogonal long axis views–2-chamber, 4-chamber, and 3-chamber or left ventricular outflow tract views.** (For the analysis of global cardiac structure and function, regional wall motion, and the calculation of volumes and mass. NOTE: Also refer to "LV Structure and Function" module as described in the Protocols section of the Appendix) (Case 1).
3. **Delayed-enhancement images spatially matched to the cine images.** (For the evaluation of myocardial infarction and viability, and tissue characterization. This corresponds to the "Late Gadolinium Enhancement" module listed in the appendix) (Case 3).

At some centers, stress perfusion imaging using adenosine has become so commonplace as to become a part of the standard examination.[1–3] Thus, this will represent the first proposed modification. The standard examination would begin as usual and proceed through the acquisition of Cine images. At this point, the patient is moved partially out of the magnet to improve visibility during the administration

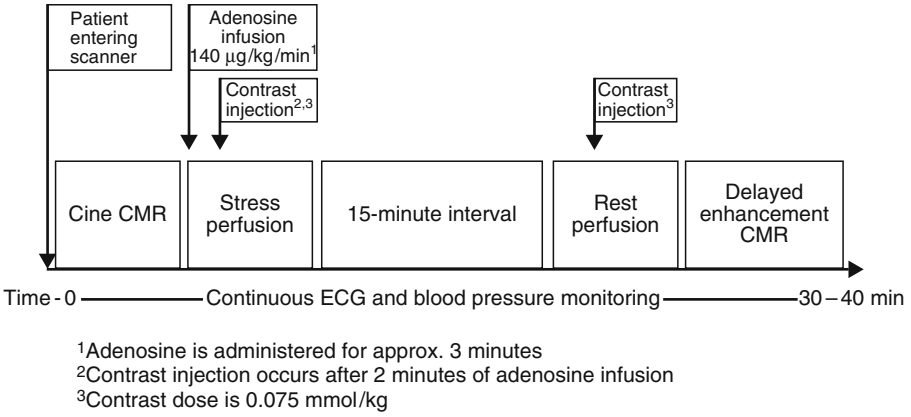

FIGURE 2.1. Timeline for adenosine stress perfusion MR

of adenosine. Adenosine is administered at a dose of 140 ug/kg/min, for at least 2 minutes, at which time the patient is then returned to the scanner bore. Contrast is then administered (dose, 0.075–0.1 mmol/kg body weight) followed by a saline flush (~50 ml) at a rate of at least 3 ml/sec via an antecubital vein. On the console, the perfusion images are observed as they are acquired, with breath-holding starting from the appearance of contrast in the right ventricular cavity. If the scanner software does not provide real-time image display, breath-holding should be started no more than 5–6 seconds after beginning gadolinium injection. Breath-holding is performed to ensure the best possible image quality (i.e. no artifacts due to respiratory motion) during the initial wash-in of contrast into the LV myocardium. Once the contrast bolus has transited the LV myocardium, adenosine is stopped and imaging is completed 5–10 seconds later. Typically, the total imaging time is 40–50 seconds, and the total time of adenosine infusion is 3 to 3.5 minutes. During vasodilation, direct access to the patient is limited only during imaging of the first pass.

Prior to the rest perfusion scan, a waiting period of about 15 minutes is required for contrast to sufficiently clear from the blood pool. During this time, additional cine and or velocity/flow imaging for valvular or hemodynamic evaluation can be performed. Subsequently, the perfusion sequence with contrast is repeated without adenosine. Approximately 5 minutes after rest perfusion, delayed enhancement imaging can be performed. The total scan time for a comprehensive cardiac MR stress test, including cine imaging, stress and rest perfusion, and delayed enhancement is usually well under 45 minutes. The timeline is displayed in Figure 2.1 (Case 25).

Obviously, different clinical circumstances will result in appropriate modification of the basic cardiac MR examination, with additional modules added as needed. For example, in patients with angina referred for stress perfusion imaging from the emergency department, if this is their first evaluation, we typically add tomographic imaging of the entire chest. Single-shot dark-blood and/or bright-blood morphological imaging is performed to obtain an overview of the great vessels and juxtacardiac structures in recognition of the fact that chest pain is not always cardiac in origin. {Case 66, series 2 and 3}

Likewise, if a stenotic aortic valve is incidentally discovered during the core exam, velocity-encoded images through the aortic valve can be added. In the setting of congenital heart disease, MR angiographic images are frequently added to the standard morphologic images, and velocity-encoded flow studies are also usually necessary in this setting. Proposed standard protocols for a variety of cardiac disorders are included in the appendix.

Interpretation and Reporting

For general clinical reporting, we use the 17-segment model recommended by the American Heart Association.[4] This model divides the basal and mid-cavity levels into 6 segments each, an apical level into 4 segments and the true apex into 1 segment (Figure 2.2). For each segment, left

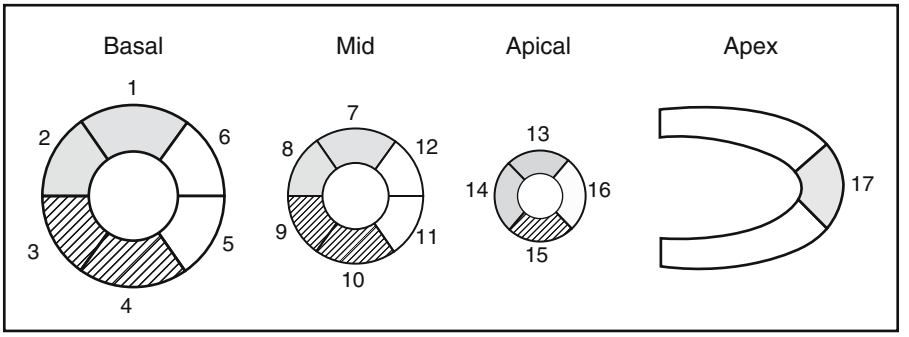

Cine Wall Motion:	Delayed Hyperenhancement:
0 = Normal/Hyperkinetic	0 = None
1 = Mild/Moderate Hypokinesis	1 = 1-25%
2 = Severe Hypokinesis	2 = 26-50%
3 = Akinetic	3 = 51-75%
4 = Dyskinetic	4 = 76-100%

FIGURE 2.2. Visual interpretation of cine and delayed enhancement images using the 17-segment model

ventricular systolic function is graded visually using a 5-point scale ranging from normal wall motion to dyskinesis. LV ejection fraction is also provided, and estimated from visual inspection of all the short- and long-axis views. Occasionally, LVEF is quantitatively measured by planimetry, such as in patients undergoing chemotherapy with potentially cardiotoxic agents.

The delayed enhancement images are also interpreted using a 5-point scale.[5] For each segment the area or transmural extent of hyperenhanced tissue is graded visually. Examples of myocardial segments with various transmural extents of hyperenhancement are shown in Figure 2.3. It is important that the delayed enhancement images are interpreted with the cine images immediately

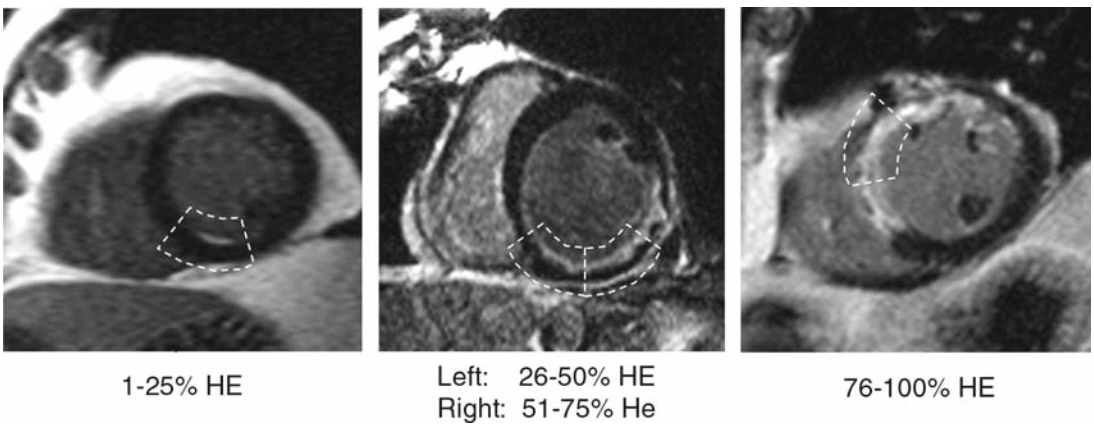

FIGURE 2.3. Typical images showing myocardial segments *(dashed white lines)* with various transmural extents of hyperenhancement. (From *J Cardiovasc Magn Reson* 2003;5:505–514, with permission)

adjacent. The cine images can provide a reference of the diastolic wall thickness of each region. This will be helpful if delayed enhancement imaging is performed before there is significant contrast washout from the LV cavity, and there is difficulty in differentiating the bright signal from the LV cavity from hyperenhanced myocardium (Figure 2.4).

Stress and rest perfusion images are scored for perfusion defects in 16 segments (segment 17 at the apex usually is not visualized). Then, a systematic stepwise approach is used to determine the presence or absence of coronary artery disease. Importantly, we use an interpretation algorithm that includes data from delayed enhancement imaging to improve the accuracy of detecting coronary artery disease over that of perfusion imaging alone (Figure 2.5).[3] Using this interpretation algorithm, a CMR stress test is deemed "positive for CAD" if myocardial infarction is present on DE-MRI ***OR*** if perfusion defects are present during stress imaging, but absent at rest ("reversible" defect) in the absence of infarction. Conversely, the test is deemed "negative for CAD" if no abnormalities are found (e.g. no MI and no stress/rest perfusion defects) ***OR*** if perfusion defects are seen at both stress and rest imaging ("matched" defect) in the absence of infarction. In the latter, matched defects are regarded as artifacts and not suggestive of CAD. When both DE-MRI and stress perfusion MRI are abnormal, the test is scored positive for ischemia if the perfusion defect is larger than the area of infarction.

The interpretation algorithm is based on two simple principles. First, with perfusion MRI and DE-MRI, there are two independent methods to obtain information regarding the presence or absence of myocardial infarction (MI). Thus, one method could be used to confirm the results of the other. Second, DE-MRI image quality (e.g. signal-to-noise ratio) is far better than perfusion MRI since it is less demanding in terms of scanner hardware (DE-MRI images can be built up over several seconds rather than in 0.1 seconds as is required for first-pass perfusion).[3] Thus, DE-MRI should be more accurate for the diagnosis of MI,[3] and the presence of infarction on DE-MRI favors the diagnosis of CAD, irrespective of the perfusion MRI results. Conceptually, it then follows that perfusion defects that have similar intensity and extent during both stress and rest ("matched"

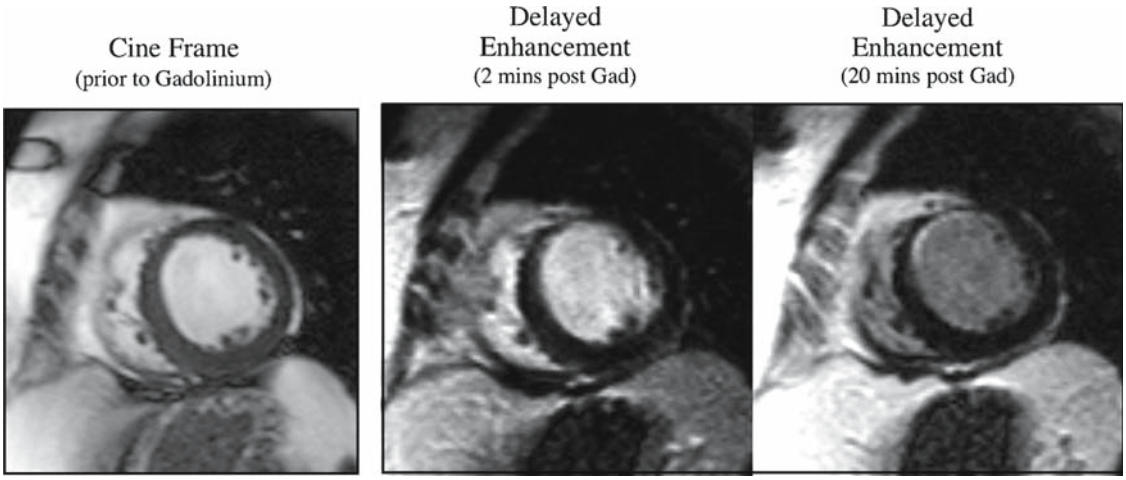

FIGURE 2.4. Short-axis view of a patient with an anterior wall myocardial infarction. Diastolic still-frame taken from the cine images before gadolinium administration is compared to the delayed enhancement image taken both early and late following gadolinium injection. Note that it is difficult to differentiate the bright LV cavity from the subendocardial infarction in the early (2 mins) delayed enhancement image. The cine frame, by showing the diastolic wall thickness in the anterior wall, provides evidence that there is subendocardial hyperenhancement in the anterior wall on the early delayed enhancement image. The late (17 mins) delayed enhancement image provides confirmation that there is subendocardial hyperenhancement in the anterior wall. (From, *J Cardiovasc Magn Reson* 2003;5:505–514, with permission)

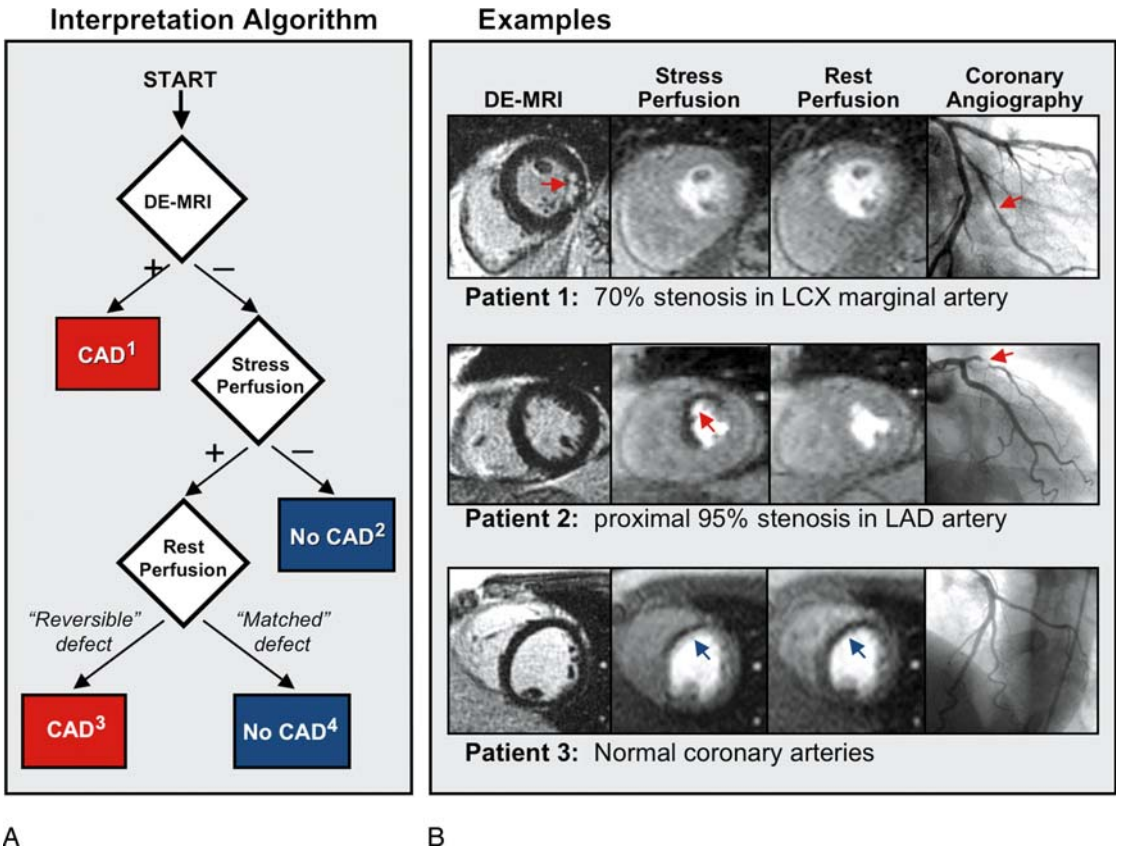

FIGURE 2.5. Interpretation algorithm for incorporating delayed enhancement imaging (DE-MRI) with stress and rest perfusion MRI for the detection of coronary disease. **(A)** Schema of the interpretation algorithm. **(1)** Positive DE-MRI Study: Hyperenhanced myocardium consistent with a prior myocardial infarction (MI) is detected. Does not include isolated midwall or epicardial hyperenhancement which can occur in nonischemic disorders. **(2)** Standard Negative Stress Study: No evidence of prior MI or inducible perfusion defects. **(3)** Standard Positive Stress Study: No evidence of prior MI but perfusion defects are present with adenosine that are absent or reduced at rest. **(4)** Artifactual Perfusion Defect: Matched stress and rest perfusion defects without evidence of prior MI on DE-MRI. **(B)** Patient Examples. **Top row:** Patient with a positive DE-MRI study demonstrating an infarct in the inferolateral wall (red arrow) although perfusion MRI is negative. The interpretation algorithm (step 1) classified this patient as positive for CAD. Coronary angiography verified disease in a circumflex marginal artery. Cine MRI demonstrated normal contractility. **Middle row:** Patient with a negative DE-MRI study but with a prominent reversible defect in the anteroseptal wall on perfusion MRI *(red arrow)*. The interpretation algorithm (step 3) classified this patient as positive for CAD. Coronary angiography demonstrated a proximal 95% LAD stenosis. **Bottom row:** Patient with a matched stress-rest perfusion defect *(blue arrows)* but without evidence of prior MI on DE-MRI. The interpretation algorithm (step 4) classified the perfusion defects as artifactual. Coronary angiography demonstrated normal coronary arteries. CAD=coronary artery disease. (Modified from Klem et al, *Circulation* 2006;47:1630–1638)

defect) but do not have infarction on DE-MRI are artifactual and should not be considered positive for CAD (with rare exceptions[2]). Concerning this latter point, it is important to recognize that the interpretation of stress/rest perfusion MRI is NOT analogous to stress/rest radionuclide imaging. For instance, "matched" defects on perfusion MRI are far more likely to represent artifact than prior myocardial infarction. Additionally, infarcted regions—particularly those that are large and transmural—often appear "reversible" on perfusion MRI. This is because infarcted regions will accumulate the